Florin Rosca*

Department of Radiation Oncology, Massachusetts General Hospital, Danvers, Massachusetts 01923, USA

***Corresponding authors:** Florin Rosca, Department of Radiation Oncology, Massachusetts General Hospital, Danvers, Massachusetts 01923, USA
E-mail: frosca@partners.org

Check for updates

Research Article

A novel film calibration method, applied to stereotactic cone commissioning

Abstract

Purpose: To present a film calibration technique that uses a few stereotactic cone irradiations on a single strip of film to generate the cone's dose profile, and its application to the commissioning of stereotactic cones in radiation oncology.

Method: In the proposed method, several radiation patterns of a stereotactic cone on a strip of film can be used to generate the cone's dose profile without any previous knowledge of film calibration. Many more calibration points were generated, in addition to those from the irradiation pattern centers, by using the fact that the irradiation patterns are generated from the same cone and hence have the same dose profile. The generated calibration curve is used to determine the cone dose profile on a relative scale. An Exradin A16 stereotactic ion chamber was used to measure the output factors and to scan the dose profiles for all our 6 cones, from 4mm to 15mm. The A16 correction convolution factor was determined by comparing the film measured profiles with the A16 scanned ones and was applied to determine the corrected absolute output factor for the 15mm cone. As both the dose profile and output factor of the 15mm cone are determined, the 15mm cone irradiation pattern becomes the calibration pattern for all subsequent commissioning measurements of profiles and absolute output factors.

Results: The method was applied to three types of film and three Monitor Unit (MU) ranges and generated dose profiles with a variation within 1% for all 6 cones. The simulations introducing noise in the film scanned image show that even with levels of noise much higher than experimentally observed, the 95% confidence level for the absolute mean/maximum variation for the generated dose profiles is below 1.6%/2.8%. The A16 convolution kernel FWHM (Full width at half maximum) generated by comparing the film and A16 dose profiles for all 6 cones falls within the narrow range of 2.07±0.1mm. The A16 convolution kernel was used to determine the A16 volumetric averaging correction for the 15mm cone output factor to be 0.4%, adjusting the A16 measurement of 0.906 to the final absolute output factor of 0.91 cGy(centigray)/MU(monitor units). The film generated output factor for the 4, 6, 7.5, 10, 12.5, and 15mm were 0.64, 0.75, 0.793, 0.863, 0.884, and 0.91, which are within 1.5% from the corrected values of the A16 measurements for cones 7.5mm and wider.

Conclusion: The described method uses a few stereotactic cones irradiations on a single strip of film to generate both the film calibration curve and the cone's dose profile, bypassing some of the inherent uncertainties associated with film dosimetry. It is a very simple method for film calibration and for determining the convolution kernel for any stereotactic detector, enabling a straight forward commissioning process for stereotactic cones and any narrow beam irradiation systems like electron and proton scanning beam.

Introduction

The accurate dosimetric characterization of small radiation fields is a stringent requirement for SRS (stereotactic radiosurgery) planning in radiation oncology. The dosimetry of small fields is challenging due to factors like the loss of lateral electronic equilibrium [1], energy dependence and fluence perturbation of detectors that are not water equivalent [2,3] and detector volume averaging. Pappas, *et al.,* [4], describe the ideal detector for small-field dosimetry as being water equivalent

and having a sufficiently small sensitive volume to avoid volume averaging. EBT2 and EBT3 (International Specialty Products, Wayne, NJ, USA) gafchromic films are becoming the detector of choice for small field dosimetry [2,5-8], since it meets the stated requirements, and provide a two-dimensional map of measured dose while requiring no chemical processing.

The usual procedure for gafchromic film calibration is to scan a piece of blank film first by placing the film in the landscape direction on the scanner, cut it into several small pieces [9-14] and exposing each film piece to a dose ranging from around

20 to 300 cGy, generating several calibration points. A PDD (Percentage Depth Dose) method for film calibration [15,16], was also proposed. Both methods use radiation patterns on sheets of film to generate a calibration curve for the entire batch of film and are affected by inaccuracies due to post-irradiation time dependence [15-18], light sensitivity [9-19], inter-sheet non-uniformity, and variations in scanning conditions.

The developed a method is trying to offer an alternative to the above-mentioned film calibration methods for stereotactic cones by generating the film calibration and cone dose profiles by using a single strip of film with 4 to 6 cone patterns.

Materials and Methods

The purpose of the presented method is to commissioning the Brainlab (Brainlab, Germany) stereotactic circular applicators, sizes 4mm to 15mm, to be used for SRS treatments. All measurements are taken with the 1000MU/min (monitor unit/minute) 6 MV (megavolt) beam from a Novalis TX linear accelerator (Varian Medical Systems, Palo Alto, USA). The output of the linear accelerator is defined as 1cGy/MU at dmax depth (1.5cm for the 6MV beam) and 100cm SSD (source to skin distance). The EBT3 gafchromic film used for output factor measurements was placed between slabs of solid water at 1.5cm depth and 98.5cm SSD, per Eclipse cone commissioning recommendations. The X and Y collimator jaws were set to 2cm for all cones.

The EBT3 film was cut in 2x10 inches strips and exposed to five stereotactic cone irradiation patterns. The cone patterns were equidistant, about 2 inches apart. Multiple cone patterns were placed on the same film without the issue of dose crosstalk due to the very low dose outside the irradiation pattern: 0.6% of maximum value an inch from the 15mm cone center and lower for the smaller cones. An Epson Expression 10000XL scanner was used for film scanning. The strips of film were placed in the center of the scanning area, parallel to the scanner lamp movement axis in order to minimize scanner non-uniformity, which is a concern mostly in the direction perpendicular to the scanning motion [20]. As mentioned in literature [21,22], scanning in reflexive mode resulted in less noisy images and hence all scanning measurements were made in reflexive mode. The images were taken with 150 dpi resolution, without color correction and saved in .tif format. The films were scanned both in 16 bits gray scale and in color rgb 48 bit scale. Since the green channel generated more consistent and less noisy results compared to the red channel and gray scale, it was used to generate the presented data. Since the analysis is limited to only one piece of film, the scale and transformations of film response have no impact on the resulting dose profiles as all patterns on it are similarly affected.

Methods

In the proposed method, several radiation patterns of the same stereotactic cone on a strip of film can be used to generate the cone dose profile without any previous knowledge of film calibration. This is possible due to the fact that the irradiation patterns are generated from the same stereotactic cone and hence have the same dose profile, scaled by the number of MUs

used for each. The generated dose profile is on an arbitrary scale and a point of known absolute dose on the pattern, is needed to generate the absolute scale.

In our case, the 15mm Brainlab stereotactic cone is used as the radiation pattern for calibration of EBT3 gafchromic film. The 15mm cone was chosen because its output factor is easier to measure using stereotactic detectors than that of smaller cones. Five 15mm cone irradiations of different MUs (40, 80, 120, 160, and 200) on a strip of film are used to generate the dose profile for the selected stereotactic cone. An in-house designed software generates a radial film response profile for each pattern with a resolution of 0.25mm.

The generation of additional calibration points

Three film radial response profiles (generated using 200, 120, and 40MUs) are displayed in Figure 1 for a 10mm cone. The film response scale is shifted and rescaled so that the 200MUs pattern spans a range between 0 and 1.

The maximum dose for the three dose profiles would be 1.0, 0.6 and 0.2, defined by the ratio of MUs used to generate them. The novel part of the presented method is to use the fact that the 5 patterns (only 3 displayed in Figure 1 for clarity) are generated by the same dose distribution, scaled by the amount of used MUs, to generate additional film calibration points.

Figure 1 displays three of the five film response radial profiles for the 10mm cone for 40, 120, and 200 MUs to describe the process of generating the additional calibration points. A horizontal line drawn from the maximum/center of the second radial profile will intersect the first radial profile at point "1A" and defines a new point of known dose on the cone dose profile: dose equal to the second pattern maximum dose (0.6) and radial distance equal to the radial coordinate of the intersection point labeled "1A". This is not a new film calibration point since it has the same dose and film response as the maximum of the second radial profile. The vertical line
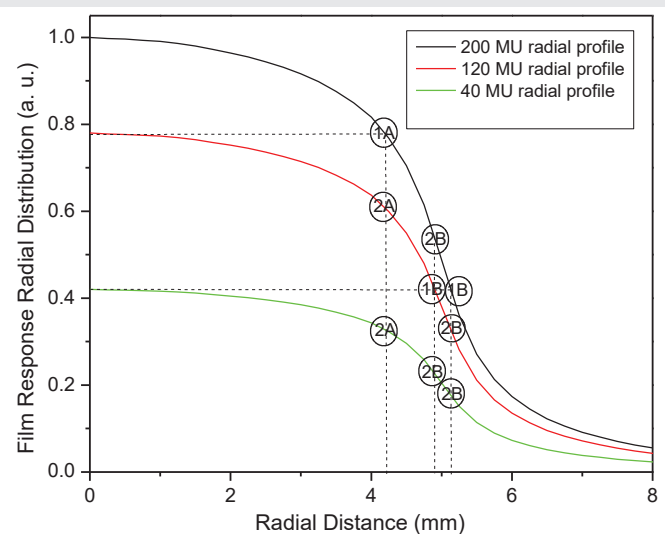
Figure 1: The figure displays three of the five film response radial profiles for the 10 mm cone for 200MU (black), 120MU (red), and 40MU (green) and describes the method for generating "secondary calibration points".

from point "1A" intersects the lower profiles in 2 points at the same radial distance defining 2 new "secondary" calibration points, labeled "2A". Their dose is determined by scaling the dose at point "1A" (0.6) to the corresponding points on the lower profiles (times 0.6 and 0.2 respectively) to get values of 0.36 and 0.12. These are two new film calibration points, having the film response values of the two "2A" points and the above determined dose. Repeating the process, the horizontal line drawn from the maximum of the third radial profile will intersect the first and second radial profiles at two points labeled "1B", defining two new points of known dose (0.2) on the cone pattern dose profile. The vertical lines from the two points "1B" intersect the other two profiles in 2 points each, defining 4 new "secondary" calibration points, labeled "2B" in Figure 1. So, starting with three film response profile and three point of known dose, we generated six more calibration points. It can be shown that if N cone patterns are used (N−1)×(N−1)×N/2 "secondary" calibration points are generated, 40 in our case of 5 patterns and 75 for 6 patterns.
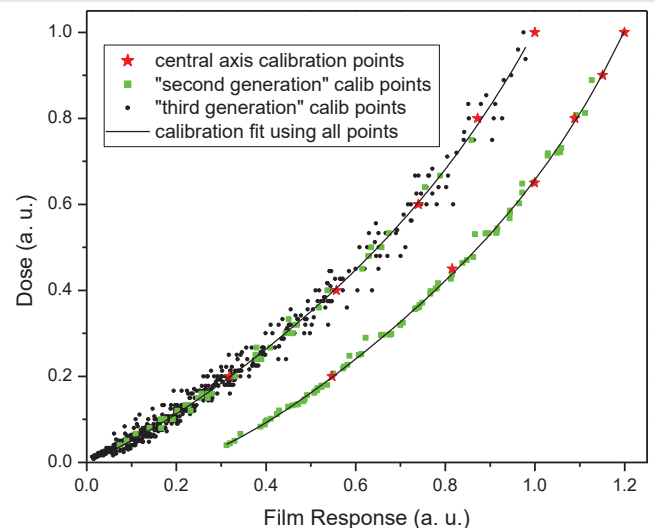
The "secondary" calibration points can become the seeds for generating a next set of calibration points just as the original 5 calibration points generated the "secondary" calibration points. The next set would contain a very high number of "tertiary" calibration points. A third order polynomial function is used to fit the calibration points and to generate the film calibration curve.

The generated film calibration curve is applied to the five patterns of different MUs to generate a dose profile for each of them. A weighted average of the five dose profiles is used to generate the final dose profile, with the used MUs as weight of the average. At this point, the cone dose profile is generated on an arbitrary scale, from one trip of film and no previous calibration information.

Results

The first calibration curve in Figure 2 displays the 5 original calibration points (generated using 200, 160, 120, 80, and 40 MUs) with red star symbols, the "secondary" calibration points with green square symbols and the "tertiary" calibration points with smaller black circular symbols. The high number of "tertiary" calibration points, especially at low response/dose, can be observed. It can also be observed that the "tertiary" calibration points have a higher spread/noise, probably since the noise in the scanned film image accumulates with each calculation step that generates the "secondary" and then "tertiary" calibration points. The film calibration curve is displayed by a black line.

Since for patterns with equally spaced MUs most additional calibration points are generated in the lower dose range, a second calibration film with a higher density of primary calibration points in the high dose range is designed to generate a more uniform distribution of calibration points. The second calibration curve in Figure 2, shifted by 0.2 to the right for viewing purposes, is generated using six 10mm cone patterns with MUs in a 0.2, 0.45, 0.65, 0.8, 0.9, and 1.0 ratio. Tertiary calibration points are not displayed since there

Figure 2: The figure displays the primary, secondary, and tertiary calibration points along with the fit that generates the film calibration curve for a five 15mm cone pattern. A second set of primary and secondary calibration points along with the film calibration curve is displayed shifted by 0.2, generated from six 10mm cone pattern. Both axes have arbitrary units.

are plenty (75) of secondary calibration points to generate a good fit/calibration curve. As expected, this MU ratio generates a more uniform density of calibration points, suggesting that choosing higher MUs for more calibration patterns could generate a more reliable fit/calibration curve. Most of the presented work though is based on the five 15mm cone patterns with equidistant MUs calibration and including the "tertiary" calibration points in the calibration curve fit.

Generation of the absolute output factor for the 15mm cone

The only step left for the generation of an absolute dose scale for the 15mm cone dose profile, that will be used for the absolute film calibration, is to measure its absolute output factor. Two methods were used for this purpose. First, the 15mm cone film response (at 1.5cm depth and 98.5cm SSD) was compared to the machine calibration conditions (1.5cm depth and 100cm SSD) on separate pieces of film, trying to find the MU ratio that results in the same film response for both patterns. This approach resulted in an output factor of 0.91±0.01 cGy/MU. This method can be used for any cone size.

For the second method an Exradin A16 stereotactic ion chamber (Standard Imaging, Middleton, WI) was used to measure the output factor and scan the profile of the 15 mm cone. The A16 measurement of the 15mm cone output factor is 0.906 cGy/MU. In order to generate the absolute output factor for the 15 mm cone from the A16 measurement the spatial convolution kernel for the A16 ion chamber was determined and used it to adjust the A16 measurement. The convolution factor has been shown to be accurately modeled by a Gaussian distribution

[23]. A Gaussian convolution factor $-\exp(-(x^2 + y^2)/a^2)-$ was applied to the film generated 2D profiles and rescaled them back to a maximum value of 1 until the optimal value of a that minimizes the chi squared difference between the film profiles after the convolution and the A16 measured profiles

for each of the 6 stereotactic cones was found. It is reassuring that the convolution kernel FWHM generated for all 6 cones, presented in Table 1, second column, falls within the narrow range of 2.07±0.1mm. The determined FWHM is similar to the 2.3mm one (estimated from Figure 2) determined by Pappas, *et al.*, [23], for the PinPoint air ion chamber (PTW, model 31006, 0.015cm³) in a 5mm diameter X-knife 6 MV beam.

The corrective factor was used to generate an estimate of the cone output factors (Table 1, fifth column) from the A16 measured output factors (Table 1, fourth column). The convolution factor for the 15mm cone was used to adjust the A16 measurement from 0.906 to 0.91 cGy/MU, which is now accepted as the absolute output factor for the 15mm cone. As expected, the corrective factor for the A16 measured output factors is small (-0.4%) for the large 15mm cone and increases for the smaller ones –16.5% for the 4mm cone. These convolution corrective factors are acceptable only for cones for which they are smaller than 3% (7.5–15mm cones) since the error in determining them is also small. Indeed, the corrected A16 values (Table 1, column 5) differ from the film measurements (Table 1, column 6) by less than 1.5% for cones 7.5 to 12.5mm.

Cone output factors

The method to generate the dose profile for any cone from a strip of film is now established and the 15mm cone absolute dose profile can be used to calibrate any film measurement. Two 15mm cone calibration patterns and three instances of the cone to be measured – irradiated on the same strip of film – were used to determine the output factors for the rest of the cones. This redundancy is designed to average out some of the film inhomogeneity effect on the measurement. The MUs for the 15mm cone patterns were chosen to deliver 200cGy and 140cGy, while the MUs for the cone to be measured were chosen to deliver estimated doses of 170, 140, and 120 cGy. The calibration curve was determined from the average of the two 15mm cone profiles, and the output factor was determined as the average of the three patterns of the cone of interest.

Discussion

As the generated cone dose profile is a weighted average of the five individual dose profiles a measure of the method's accuracy can be inferred by comparing the five individual dose profiles after rescaling them to correspond to same MUs. When using the green channel for film scanning, the five dose profiles were within ± 3% from the average profile, while when using the red channel or gray scale they were within ± 5% from the average profile.

To test the reproducibility of the generated dose profiles the described method was applied to EBT3 gafchromic film using three ranges of MUs – max of 200, 400, and 600 – and to EDR2 and EBT2 films. The difference between the five dose profiles and their average is less than 1% of maximum dose, suggesting that the presented method is quite robust across types of films and MU ranges.

Error analysis

Levels of noise in the scanned film density profiles were simulated to quantify its effect on the accuracy of the generated dose profile. The known dose profile for the 1cm cone was used to generate copies of it for the number of patterns considered (4-6) by scaling them proportionally to the MUs used to irradiate the film. In the next step noise was added by rescaling each dose profile by a factor equal to a *max_resc* factor time a random number between –1 and 1, and by shifting them by an amount equal to a *max_shift* factor times a random number between –1 and 1. It should be noted that the shift part of the noise will more severely affect the low MU dose profiles. The *max_resc/max_shift* factors for the three levels of noise were chosen to be for Noise1: 2%/0.5%, for Noise2: 3%/1%, for Noise3: 2% of max /1%. For the third noise level the 2% rescale is taken out of the maximum profile amplitude instead of out of each profile's amplitude, affecting the lower MU profiles more severely. For the considered 5 cone pattern, using MU ratio of (1, 0.8, 0.6, 0.4, 0.2), the introduced noise levels generate maximum variations of (±2.5%, ±2.625%, ±2.83%, ±3.25%, ±4.5%) for Noise1, (±4%, ±4.25%, ±4.67%, ±5.5%, ±8%) for Noise2, and (±3%, ±3.75%, ±5%, ±7.5%, ±15%) for Noise3, out of each profile's amplitude. The Noise1 level more closely resembles the variation observed in the experimentally generated dose profiles, while cases 2 and 3 are clearly higher.

The such generated "noisy" dose profiles are converted into "noisy" film density profiles using a known dose-to-film density calibration curve and used as the starting point for the described analysis. This simulation was run for 4, 5, and 6 cone patterns per film. For each number of patterns per film the analysis was performed using only the calibration points at the center of the cones (1, primary), the primary and secondary calibration points generated as described by the method (1+2), and finally, using the primary, secondary and

Table 1: The table contains the FWHM (Full width at half maximum) of the optimal convolution factor for the A16 ion chamber for each cone (column 2), the correction to the measured output factors (column 3), the A16 measured cone output factors (column 4), the corrected output factors (column 5), and the cone output factors generated using film measurements.

Cone Size (mm)	FWHM (mm)	Correc. Factor	A16 meas.	A16 deconv.	Film meas.
4	1.97	0.835	0.51	0.611	0.64
6	2.0	0.952	0.69	0.725	0.75
7.5	2.06	0.977	0.77	0.788	0.793
10	2.09	0.985	0.84	0.853	0.863
12.5	2.15	0.993	0.89	0.896	0.884
15	2.16	0.996	0.906	0.91	0.91

tertiary calibration points (1+2+3). For the primary calibration points–only analysis a "zero" dose calibration point had to be added to be able to generate a full calibration curve in the low dose region. An absolute difference between the initial dose profile and the one generated by the analysis of the "noisy" scanned film intensity profiles was calculated as a measure of the variation in the generated dose profile due to film noise. Each analysis was run 1000 times and a 95% confidence level was determined for the absolute mean/maximum difference between the initial and final dose profiles. The absolute mean/max differences are presented in Table 2 in percentage.

The absolute mean/max error of the generated dose profile decreases with increasing number of patterns, since more cone patterns contain more information and hence more noise averaging. Secondly, adding secondary and tertiary calibration points to the analysis increased the accuracy of the final dose profile, dramatically so for the 4 pattern case. It is remarkable that even with a much higher than experimentally observed level of noise added, the 95% confidence level for the absolute mean/max variation is below 1.6% / 2.8% for the 4 patterns case, and below 1.3% / 2.5% for the 5 or 6 patterns case if the analysis includes the primary, secondary and tertiary calibration points. These uncertainty levels are similar or smaller (especially for the realistic case 1 noise) compared to the 1.1% to 2.1% range reported by Papaconstadopoulos, *et al.*, [22], or with the 2% 2mm gamma criteria used by Chang, *et al.*, [15].

Conclusion

A method of film calibration that uses stereotactic cones and generates the cone's dose profile from one strip of film with a few irradiations was described. To place the dose profile on an absolute scale the output factor of the 15 mm cone was measured, using both film and the A16 ion chamber. The determined absolute dose profile of the 15mm cone are used for film calibration for all the measurements required for the stereotactic cone commissioning.

The described method can be translated to the commissioning of any narrow beam irradiation systems like electron and proton scanning beam. It can also be generalized to calibration of other planar detectors–portal vision panels for example–by using appropriately designed irradiation patterns, not necessarily from stereotactic cones. Such a simple method of stereotactic cone commissioning could enable treatment planning system companies to take a more active role in overseeing the quality of data used to commission their systems. A few strips of film containing the determination of the calibration dose profile, output factors, and TMR check points can be scanned and sent, along with some output factors and dose profiles measured with a stereotactic detector. Such oversight would reduce the large variability in data associated with the challenging measurement of narrow stereotactic beams.

Table 2: The 95% confidence level for the simulated dose profiles for the absolute mean and maximum difference between the original dose profile and those generated from the simulated "noisy data". The absolute mean/max differences are in percentage. The analysis was run for 4, 5, and 6 number of patterns per film, using only the calibration points at the center of the cones (1, primary), the primary and secondary calibration points (1+2), and using the primary, secondary and tertiary calibration points (1+2+3). The noise amplitude used in the simulation increases from Noise1 to Noise3 as described in the text.

	4 patterns			5 patterns			6 patterns		
	1	1+2	1+2+3	1	1+2	1+2+3	1	1+2	1+2+3
Noise 1	3/9.4	1.8/4.8	0.8/1.6	1.3/4.3	1.2/3.4	0.6/1.3	0.7/1.8	0.8/1.8	0.6/1.2
Noise 2	4.7/14.7	3.2/8.8	1.5/2.6	2.2/6.7	1.9/4.6	1.3/2.2	1.1/3.0	1.4/2.6	1.2/2.0
Noise 3	5.8/17.6	3/7.5	1.6/2.8	3/8.5	1.9/4.9	1.3/2.4	2.4/6.1	1.4/2.9	1.3/2.5

References

1. Das IJ, Ding GX, Ahnesjö A (2008) Small fields: Nonequilibrium radiation dosimetry. Med Phys 35: 206-215. **Link:** http://bit.ly/35sSoMK

2. Aspradakis MM, Byrne JP, Palmans H, Duane S, Conway J, et al. (2010) IPEM report 103: small field MV photon dosimetry. **Link:** http://bit.ly/2QIP6AF

3. Alfonso R, Andreo P, Capote R, Huq MS, Kilby W, et al. (2008) A new formalism for reference dosimetry of small and nonstandard fields. Med Phys 35: 5179-5186. **Link:** http://bit.ly/2OAmTta

4. Pappas E, Maris TG, Zacharopoulou F, Papadakis A, Manolopoulos S, et al. (2008) Small SRS photon field profile dosimetry performed using a PinPoint air ion chamber, a diamond detector, a novel silicon-diode array (DOSI), and polymer gel dosimetry. Analysis and intercomparison. Med Phys 35: 4640-4648. **Link:** http://bit.ly/2XMdzqs

5. Butson M, Peter K, Cheung T, Hani A (2010) Energy response of the new EBT2 radiochromic film to x-ray radiation. Radiat Meas 45: 836. **Link:** http://bit.ly/37Adsmr

6. Ralston A, Liu P, Warrener K, McKenzie D, Suchowerska N (2012) Small field diode correction factors derived using an air core fibre optic scintillation dosimeter and EBT2 film. Phys Med Biol 57: 2587-2602. **Link:** http://bit.ly/2riCSEe

7. Gagnon JC, Thériault D, Guillot M, Archambault L, Beddar S, et al. (2012) Dosimetric performance and array assessment of plastic scintillation detectors for stereotactic radiosurgery quality assurance. Med Phys 39: 429-436. **Link:** http://bit.ly/2OdCsYQ

8. Hardcastle N, Basavatia A, Bayliss A, Tome WA (2011) High dose per fraction dosimetry of small fields with Gafchromic EBT2 film. Med Phys 38: 4081-4085. **Link:** http://bit.ly/2D85NgT

9. Hartmann B, Martišíková M, Jäkel O (2010) Technical Note: Homogeneity of Gafchromic® EBT2 film. Med Phys 37: 1753. **Link:** http://bit.ly/34pAkCM

10. Desroches J, Bouchard H, Lacroix F (2010) Potential errors in optical density measurements due to scanning side in EBT and EBT2 Gafchromic film dosimetry. Med Phys 37: 1565-1570. **Link:** http://bit.ly/34e6zFa

11. Andres C, del Castillo A, Tortosa R, Alonso D, Barquero R (2010) A comprehensive study of the Gafchromic EBT2 radiochromic film. A comparison with EBT. Med Phys 37: 6271-6278. **Link:** http://bit.ly/33bPPNm

12. Arjomandy B, Tailor R, Anand A, Sahoo N, Gillin M, et al. (2010) Energy dependence and dose response of Gafchromic EBT2 film over a wide range of photon, electron, and proton beam energies. Med Phys 37: 1942-1947. **Link:** http://bit.ly/2OedqsH

13. Kairn T, Aland T, Kenny J (2010) Local heterogeneities in early batches of EBT2 film: A suggested solution. Phys Med Biol 55: L37-L42. **Link:** http://bit.ly/2KLLlkQ

14. Richley L, John AC, Coomber H, Fletcher S (2010) Evaluation and optimization of the new EBT2 radiochromic film dosimetry system for patient dose verification in radiotherapy. Phys Med Biol 55: 2601-2617. **Link:** http://bit.ly/2DbpuEJ

15. Chang L, Ho SY, Lee TF, Yeh SA, Ding HJ, et al. (2015) Calibration of EBT2 film using a red-channel PDD method in combination with a modified three-channel technique. Med Phys 42: 5838-5847. **Link:** http://bit.ly/2XEpyWV

16. Ferreira BC, Lopes MC, Capela M (2009) Evaluation of an Epson flatbed scanner to read Gafchromic EBT films for radiation dosimetry. Phys Med Biol 54: 1073-1085. **Link:** http://bit.ly/33cJCkn

17. Lewis D, Micke A, Yu X, Chan MF (2012) An efficient protocol for radiochromic film dosimetry combining calibration and measurement in a single scan Med Phys 39: 6339-6350. **Link:** http://bit.ly/2sc5e3B

18. Mayer RR, Ma F, Chen Y, Miller RI, Belard A, et al. (2012) Enhanced dosimetry procedures and assessment for EBT2 radiochromic film. Med Phys 39: 2147-2155. **Link:** http://bit.ly/2QU12Qr

19. ISP (2009) Gafchromic R_ Ebt2 self-developing film for radiotherapy dosimetry

20. Menegotti L, Delana A, Martignano A (2008) Radiochromic film dosimetry with flatbed scanners: A fast and accurate method for dose calibration and uniformity correction with single film exposure. Med Phys 35: 3078-3085. **Link:** http://bit.ly/35sUfkG

21. Farah N, Francis Z, Abboud M (2014) Analysis of the EBT3 Gafchromic film irradiated with 6 MV photons and 6 MeV electrons using reflective mode scanners. Phys Med 30: 708-712. **Link:** http://bit.ly/2D9PqRe

22. Papaconstadopoulos P, Hegyi G, Seuntjens J, Devic S (2014) A protocol for EBT3 radiochromic film dosimetry using reflection scanning. Med Phys 41: 1221011. **Link:** http://bit.ly/2pHYedJ

23. Pappas E, Maris TG, Papadakis A, Zacharopoulou F, Damilakis J, et al. (2006) Experimental determination of the effect of detector size on profile measurements in narrow photon beams Med Phys 33: 3700-3710. **Link:** http://bit.ly/33eE88A